Advances in Science and Technology Research Journal

Advances in Science and Technology Research Journal, 2026, 20(6), 314–324
https://doi.org/10.12913/22998624/218005
ISSN 2299-8624, License CC-BY 4.0

Received: 2026.01.28
Accepted: 2026.04.15
Published: 2026.05.01

Abaqus-based numerical modeling of a two-layer timber beam under fully composite and fully non-composite conditions

Tuan Trong Tran[1], Quyen Bich Vu[1*], Trung-Hieu Tran[1], Hieu-Nghia Hoang[2], The-Hoan Nguyen[3]

[1] Hanoi Architectural University, 129 Tran Phu, Hanoi, Vietnam
[2] Hai Phong University, 171 Phan Dang Luu, Phu Lien, Hai Phong, Vietnam
[3] Thuc Phan Ward Administration, Cao Bang, Vietnam
* Corresponding author's e-mail: quyenvtb@hau.edu.vn

ABSTRACT

This paper presents a numerical simulation study of the elastic response of a two-layer laminated timber beam under two idealized interlayer interaction limit states, namely fully composite and fully non-composite behavior. A finite element model was developed in Abaqus, in which spruce wood was represented using an orthotropic linear elastic constitutive model. The objective is to establish the theoretical bounds of structural response by simulating these two extreme interaction conditions within the linear elastic range. The numerical force–displacement responses obtained from the model are compared with analytical solutions derived from classical composite beam theory, showing close agreement at the global stiffness level. Beyond global response comparison, stress field analysis is used to interpret interlayer force transfer mechanisms, stress redistribution, and cross-sectional mobilization under different interaction assumptions. The results demonstrate the strong influence of interlayer shear interaction on flexural stiffness and stress continuity across the section. The proposed modeling framework is intended as a numerical baseline for subsequent extensions toward connector-based partial interaction models and nonlinear analysis of laminated timber beams.

Keywords: two-layer timber beam, composite and non-composite action, interlayer shear transfer, FEA, Abaqus modeling.

INTRODUCTION

Due to its high strength-to-weight ratio, flexibility in form, aesthetic qualities, and environmental advantages over traditional inorganic materials like concrete and steel, glued laminated timber, or glulam, has been utilized in European construction since the late nineteenth century [1] and has grown in recognition as an effective structural material in contemporary engineering applications [2]. However, life-cycle inventory (LCI) studies show that a significant amount of energy is still needed to produce structural timber [3], underscoring the need to maximize the use of natural resources to maintain the environmental advantages of timber at the structural level. Enhancing the composite action between timber layers in laminated beams by examining how structural configuration and interlayer interaction circumstances affect the overall mechanical response is one practical solution to this problem.

Developments in finite element method (FEM) modeling have coincided with breakthroughs in timber structural engineering by offering potent tools for precisely capturing stress distributions in orthotropic materials and assessing the elastic behavior of timber structures. While Feio et al. [5] used a combination of numerical and experimental methods to forecast stiffness and internal stress distributions in conventional timber joints, Xu et al. [4] created a three-dimensional FEM model for timber joints subjected to parallel-to-grain loading. At the structural scale, Sangree and Schafer [6] demonstrated that FEM can reliably

reproduce the elastic deformation behavior of scarf-jointed timber beams under realistic loading conditions. Beyond timber structures, advanced finite element modeling frameworks have also been widely applied to nonlinear and inelastic behavior in steel and concrete members, including local buckling of steel columns and damage plasticity modeling of reinforced concrete beams, further demonstrating the robustness and versatility of FEM-based structural analysis approaches [7–9]. Moreover, fundamental studies on material mechanics and the elastic properties of wood [10–11] confirm that representing wood as an orthotropic linear elastic material is appropriate for evaluating its elastic response.

From a theoretical standpoint, the mechanical behavior of laminated timber beams is strongly governed by the degree of shear interaction between the individual layers. Two idealized limit conditions are commonly considered: the fully non-composite state, in which the layers act independently without shear transfer, and the fully composite state, in which perfect interlayer interaction is assumed and the beam behaves equivalently to a monolithic cross-section. Analytical solutions describing these two extreme cases are well established in classical structural mechanics and provide an essential theoretical framework for the evaluation and validation of numerical models, with Möhler's theory being one of the most widely referenced approaches [12].

Based on these theoretical foundations and previous research, the present study conducts a finite element analysis to investigate the elastic behavior of a two-layer laminated timber beam without mechanical anti-slip connections between the layers. To determine the theoretical limits of the structural response, two idealized interlayer interaction conditions – completely composite and entirely non-composite – are simulated. The numerical model is developed in Abaqus, where spruce wood is described using an orthotropic linear elastic constitutive model, enabling an accurate representation of load transfer and deformation mechanisms within the beam. The numerically obtained force-displacement responses are compared with analytical solutions derived from Möhler's theory [12], while stress field analysis is employed to elucidate the influence of interlayer interaction on bending stiffness and stress distribution in two-layer laminated timber beams.

It should be emphasized that the objective of this study is not limited to verifying analytical solutions using a commercial finite element tool. Rather, the work establishes a consistent and reproducible numerical modeling framework that enables displacement-consistent comparison between different interlayer interaction states and provides detailed mechanistic insight into stress redistribution, layer-wise force transfer, and cross-sectional mobilization – quantities that cannot be directly obtained from classical analytical formulations. This framework is intended to serve as a baseline for subsequent nonlinear and connector-based modeling extensions of laminated timber systems.

NUMERICAL MODEL

Theoretical aspect

The elastic strain $\underline{\varepsilon}^e$ is reversible and can be related to the Cauchy stress $\underline{\sigma}$ by a law elastic by introducing the tensor of order 4 of the elastic constants "$\underline{\underline{\Lambda}}$":

$$\underline{\sigma} = \underline{\underline{\Lambda}} : \underline{\varepsilon}^e \tag{1}$$

For an orthotropic material, the tensor "$\underline{\underline{\Lambda}}$" is calculated by:

$$\underline{\underline{\Lambda}} = \begin{bmatrix} C_{11} & C_{12} & C_{13} & 0 & 0 & 0 \\ C_{12} & C_{22} & C_{23} & 0 & 0 & 0 \\ C_{13} & C_{23} & C_{33} & 0 & 0 & 0 \\ 0 & 0 & 0 & C_{44} & 0 & 0 \\ 0 & 0 & 0 & 0 & C_{55} & 0 \\ 0 & 0 & 0 & 0 & 0 & C_{66} \end{bmatrix} \tag{2}$$

with:

$$C_{11} = \frac{1 - \nu_{23}\nu_{32}}{\Delta E_2 E_3}; C_{22} = \frac{1 - \nu_{13}\nu_{31}}{\Delta E_1 E_3}; \quad C_{33} = \frac{1 - \nu_{12}\nu_{21}}{\Delta E_1 E_2} \tag{3}$$

$$C_{12} = \frac{\nu_{21} + \nu_{31}\nu_{23}}{\Delta E_2 E_3}; C_{13} = \frac{\nu_{31} + \nu_{21}\nu_{32}}{\Delta E_2 E_3}; \quad C_{23} = \frac{\nu_{32} + \nu_{12}\nu_{31}}{\Delta E_1 E_3} \tag{4}$$

$$C_{44} = 2G_{12}; C_{55} = 2G_{13}; \; C_{66} = 2G_{23} \tag{5}$$

$$\Delta = \frac{1 - \nu_{12}\nu_{21} - \nu_{23}\nu_{32} - \nu_{13}\nu_{31} - 2\nu_{21}\nu_{32}\nu_{13}}{E_1 E_2 E_3} \tag{6}$$

where: E_i – Young's modulus in direction (i), ν_{ij} and G_{ij} are respectively the Poisson's ratio and the Coulomb modulus in the plane (i–j).

Background and limit models

Two theoretical limit models were formulated to define the lower and upper bounds of the elastic stiffness of laminated timber beams. These models correspond to two extreme interlayer interaction conditions and provide a rational framework for assessing the range of possible mechanical responses of the structural system.

In the fully non-composite configuration, the interface between adjacent timber layers was modeled as a frictionless contact in Abaqus to permit unrestricted relative sliding under bending action. A surface-to-surface contact formulation was adopted with frictionless tangential behavior (friction coefficient $\mu = 0$) and hard contact in the normal direction to prevent interpenetration while allowing free tangential slip. Under this assumption, no shear transfer occurs across the interface, and each layer behaves as an independent structural member without mechanical interaction with the neighboring layer. The global beam response in this limit case can therefore be interpreted as the superposition of the individual layer responses, corresponding to the minimum attainable flexural stiffness of the system. Consistent with this modeling assumption, discontinuities in the interfacial stress distribution are observed, which are characteristic of fully non-composite behavior.

In contrast, the fully composite configuration assumes a perfectly bonded interlayer interface, ensuring full displacement compatibility along both the beam length and the entire contact surface. According to this theory, shear stresses are fully transferred over the interface, causing the timber layers to deform simultaneously and behave as a single monolithic cross-section. In the finite element implementation, this condition is realized in Abaqus by applying a surface-based tie constraint at the interlayer contact interface, which enforces equality of translational degrees of freedom between the two layer surfaces and prevents both relative tangential slip and normal separation. This interaction mechanism results in the highest theoretical elastic stiffness of the beam and facilitates the effective mobilization of the entire cross-section during bending. The continuous distribution of the stress field across the cross-section depth in this instance amply illustrates the coordinated involvement of every layer in the load transfer process.

In addition to establishing the theoretical limitations of elastic stiffness, taking into account these two limit states offers a crucial foundation for the verification and calibration of numerical models. Since the actual behavior of laminated timber beams in practical applications generally lies between these two extremes, the formulation and analysis of fully non-composite and fully composite models are essential for evaluating the degree of interlayer interaction and for elucidating its influence on the elastic response of laminated timber beam systems.

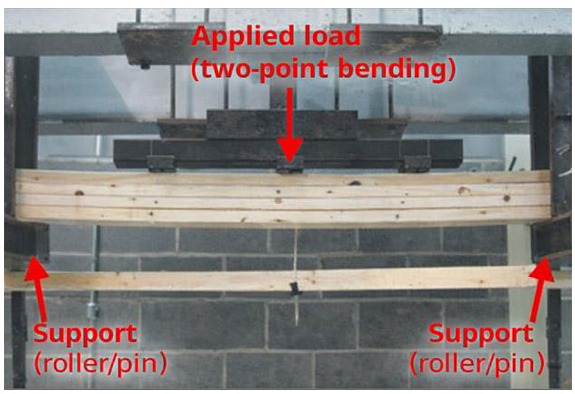

Figure 1. Four-point bending test setup of the multi-layer laminated timber beam during loading [13]

SIMULATION RESULTS AND ANALYSIS

Testing configuration

Four-point bending tests (Figure 1) were performed to characterize the elastic response of laminated timber beams and to provide reference data for the calibration and validation of the numerical model. The testing protocol and loading arrangement were established in accordance with the procedures reported by O'Loinsigh et al. [13]. All specimens were loaded monotonically within the elastic range, and the force–displacement response at mid-span was continuously recorded to evaluate the equivalent flexural stiffness.

The beams were tested under a symmetric four-point bending configuration with a total span of 2000 mm. Two loading points were applied at equal distances of 600 mm from each support, resulting in a constant bending moment region of 800 mm at the beam center. They were illustrated in Figure 2. Each timber lamina had dimensions of 140 × 38 × 2200 mm, and the layers were mechanically clamped to ensure uniform contact along the interface throughout the test.

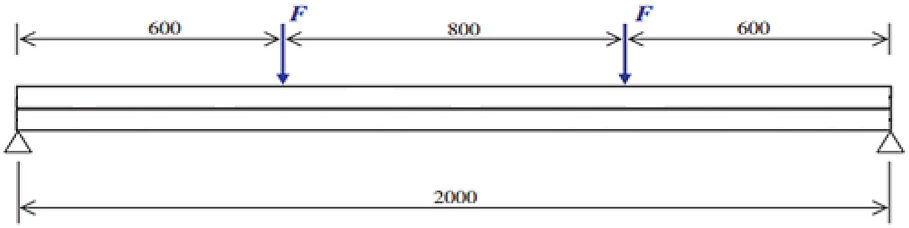

Figure 2. Schematic of the four-point bending test arrangement (dimensions in mm)

Simulation configuration

A three-dimensional finite element model of the two-layer laminated timber beam without mechanical shear connectors (Figure 3) was developed using the Abaqus software package [14] to investigate its elastic response under bending. The timber material was discretized using eight-node linear brick elements with reduced integration (C3D8R), which are well suited for modeling orthotropic linear elastic behavior and offer a good balance between computational efficiency and numerical accuracy.

To reduce computational cost while preserving the structural response, geometric and loading symmetries were exploited by introducing two symmetry planes, so that only one-quarter of the full beam geometry was modeled. This symmetry-based reduction significantly decreases the number of degrees of freedom and computational time, while maintaining the accuracy of the displacement and stress fields for the considered loading configuration. The loading and support conditions were defined consistently with this quarter-model assumption.

In Abaqus, standard symmetry boundary conditions were applied on the two symmetry planes. On the X-symmetry plane, an XSYMM constraint was imposed (U1 = UR2 = UR3 = 0), and on the Z-symmetry plane, a ZSYMM constraint was imposed (U3 = UR1 = UR2 = 0). The right support was modeled by constraining the vertical displacement only (U2 = 0), representing a simple support condition. The external action was introduced using a displacement-controlled loading scheme, in which a prescribed vertical displacement (U2 direction) was applied at the loading point through a boundary condition rather than a force-controlled load. This approach improves numerical stability in the nonlinear analysis and ensures direct correspondence with the measured load–displacement response. The finite element mesh was generated using a structured meshing strategy with a uniform element size applied over the beam cross-section and along the longitudinal direction. Eight-node linear brick elements with reduced integration (C3D8R) were used in all simulations. An extended mesh convergence study was carried out using eleven characteristic element sizes ranging from 10 mm to 20 mm, as summarized in Table 1, resulting in meshes from 440 to 3080 elements per timber layer.

Because the analysis is linear elastic and displacement-controlled, limited mesh sensitivity is expected for the global structural response. The computed load–displacement curves and characteristic stress measures show very small variation across the tested mesh densities, as illustrated in Figure 5, confirming mesh-independent behavior. Based on the convergence results, the medium mesh level (element size ≈ 13 mm, about 1.275 elements per timber layer) was selected as an appropriate compromise between accuracy and computational efficiency.

The orthotropic elastic properties assigned to the spruce layers in the finite element model were adopted directly from the experimentally characterized dataset reported in Reference [15]. These parameters are representative of structural spruce and are appropriate for linear elastic analysis. The material principal directions in the model were aligned with the wood anatomical axes, where direction 1 corresponds to the longitudinal (L) direction parallel to the grain, direction 2 to the radial (R) direction, and direction 3 to the tangential (T) direction. The complete set of elastic constants used in the simulations is summarized in Table 2.

RESULTS

Figure 4 illustrates the force–displacement response of a two-layer laminated timber beam under two idealized interlayer interaction conditions, namely fully non-composite (FNC) and fully composite (FC), and compares the finite

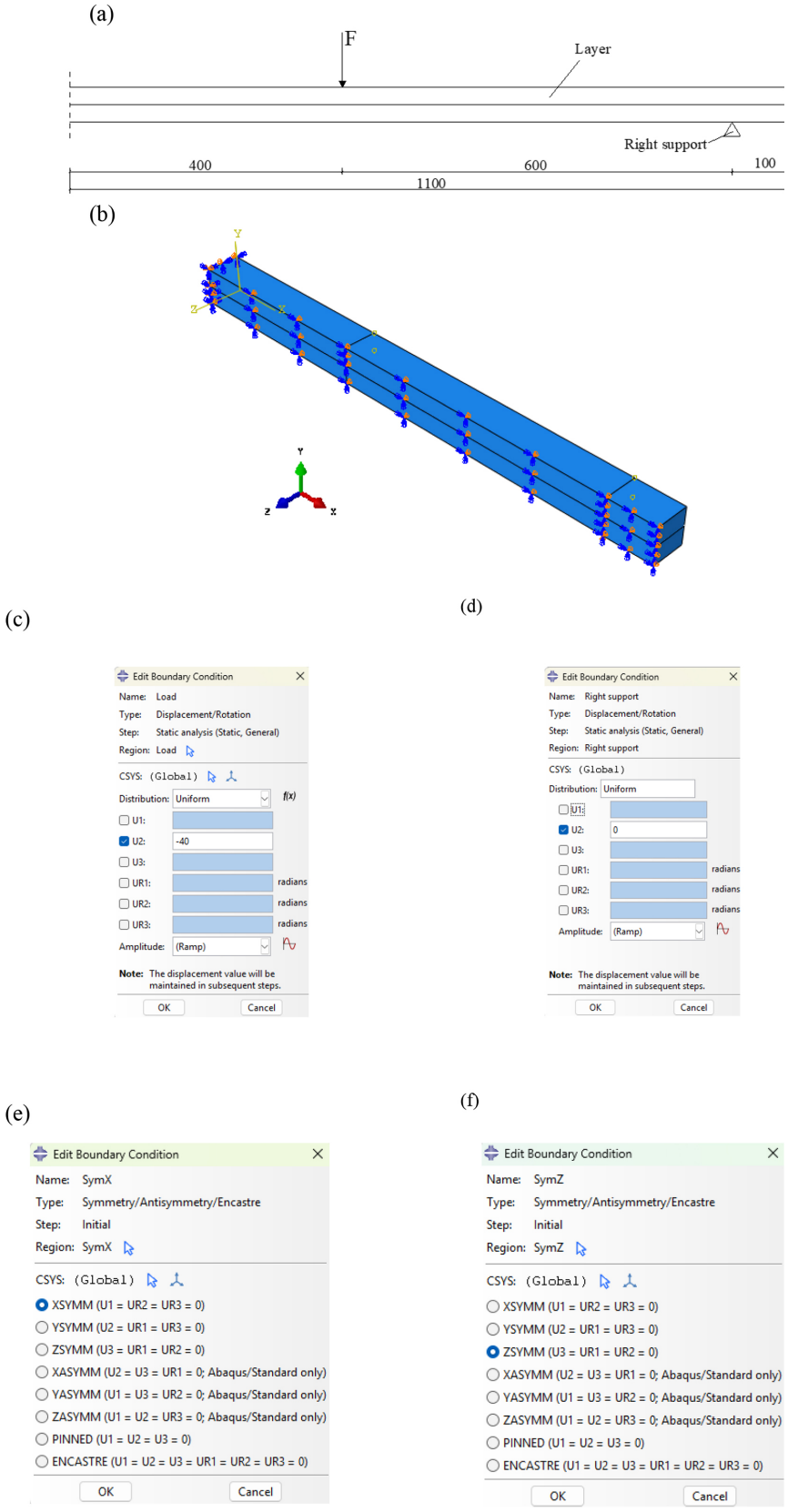

Figure 3. Finite element modeling strategy and boundary conditions for the quarter laminated timber beam model: (a) quarter-beam schematic showing layer configuration, loading position, and support location, (b) finite element model with symmetry conditions and displacement constraints, (c) displacement-controlled loading definition in Abaqus (prescribed vertical displacement at loading point), (d) boundary condition definition for the right support (vertical displacement constraint), (e) x-symmetry boundary condition (XSYMM constraint in Abaqus), (f) Z-symmetry boundary condition (ZSYMM constraint in Abaqus)

Table 1. Extended mesh convergence study using C3D8R elements with uniform element size (10–20 mm)

Mesh size (mm)	Element type	Number of elements (per timber layer)
10	C3D8R	3080
11	C3D8R	1800
12	C3D8R	1638
13	C3D8R	1275
14	C3D8R	1185
15	C3D8R	1110
16	C3D8R	552
17	C3D8R	520
18	C3D8R	488
19	C3D8R	464
20	C3D8R	440

element results with the corresponding analytical predictions. An almost perfect superposition between the numerical and theoretical curves is observed over the entire elastic range, indicating that the developed finite element model is capable of accurately reproducing the elastic response of the beam in both limiting interaction states.

The pronounced difference in the slope of the force–displacement curves highlight the dominant role of interlayer interaction in governing the global flexural stiffness of the beam. Because there is no shear transfer across the interface in the totally non-composite arrangement, the separate layers deform independently, as indicated by the lower slope. The fully composite arrangement, on the other hand, has a noticeably larger slope, which corresponds to a successful composite action where full shear transfer allows the entire cross-section to participate coherently in resisting bending. The outstanding agreement between the analytical solutions and numerical simulations justifies the proposed assumptions about orthotropic elastic material properties and interlayer interaction conditions, as well as the internal consistency of the finite element formulation. A quantitative comparison of the initial bending stiffness shows that the relative difference between the analytical and FE results is below 0.5% for the fully non-composite case and below 0.8% for the fully composite case, in addition to the near-perfect overlap of the force–displacement curves. As a result, the numerical model may be considered as consistently validated at the level of global elastic response, offering a solid basis for further numerical studies concentrating on load transfer mechanisms and stress distribution in two-layer laminated timber beams.

To further verify the numerical robustness of the finite element model, a mesh convergence study was carried out using multiple discretization levels. Figure 5 presents the load–displacement responses obtained with element sizes ranging from 10 mm to 20 mm using C3D8R elements, corresponding to the mesh configurations summarized in Table 2. All simulations were performed under the same displacement-controlled loading and boundary condition framework.

The curves corresponding to different mesh sizes are nearly indistinguishable over the entire displacement range, indicating very low sensitivity of the global structural response to mesh refinement in the considered elastic regime. Both the initial stiffness and the overall slope of the load–displacement relationship remain

Table 2. Orthotropic elastic properties of spruce used in the finite element model (from experimentally characterized data in [15])

Property	Symbol	Value	Unit	Material direction
Longitudinal modulus	E_1 (E_L)	12000	MPa	Along grain (L)
Radial modulus	E_2 (E_R)	400	MPa	Radial (R)
Tangential modulus	E_3 (E_T)	400	MPa	Tangential (T)
Poisson's ratio	ν_{12}	0.30	–	L–R
Poisson's ratio	ν_{13}	0.30	–	L–T
Poisson's ratio	ν_{23}	0.32	–	R–T
Shear modulus	G_{12}	690	MPa	L–R
Shear modulus	G_{13}	690	MPa	L–T
Shear modulus	G_{23}	50	MPa	R–T

Note: Material axes are defined as follows: direction 1 = longitudinal (L, parallel to grain), direction 2 = radial (R), and direction 3 = tangential (T). The same local material orientation was assigned to both timber layers in the finite element model.

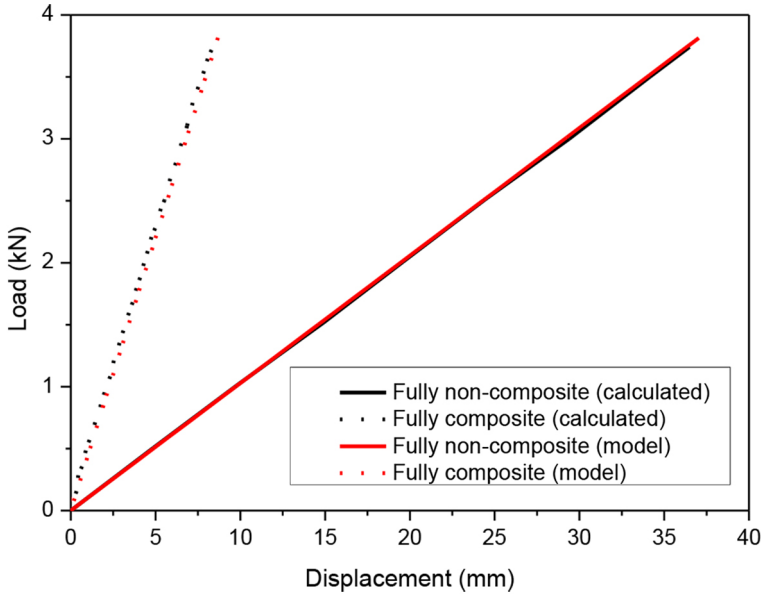

Figure 4. Force–displacement responses of two- beams under fully non-composite and fully composite conditions, comparing numerical simulation with theoretical predictions

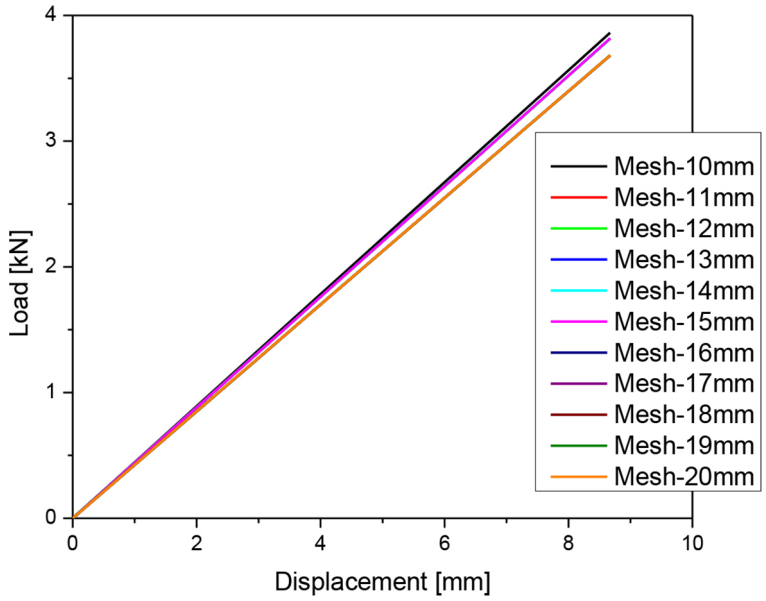

Figure 5. Mesh convergence study: load–displacement responses obtained with element sizes ranging from 10 mm to 20 mm (C3D8R elements)

essentially unchanged as the mesh is refined. The maximum deviation between the finest and coarsest meshes is minimal, confirming that the solution is mesh-independent for the response quantities of interest. This result supports the selection of the medium mesh size (13 mm) as a reliable and computationally efficient discretization for the subsequent simulations. The Von Mises stress distributions of a two-layer laminated timber beam under two idealized interlayer interaction conditions – completely non-composite (FNC) and fully composite (FC) – at various mid-span displacement levels are shown in Figures 5 and 6. The selected displacement levels (4, 6.4, and 8 mm) correspond to representative points along the elastic force–displacement response, with the fully composite case evaluated up to 8 mm in the present study. These values were chosen to illustrate the progressive evolution of the stress field with increasing elastic deformation and, at the same time, to enable a consistent comparison at identical displacement levels between the FC

and FNC configurations. These results provide clear insight into the differences in force transfer mechanisms, stress distribution characteristics, and the degree of cross-sectional mobilization associated with each interaction state, thereby highlighting the fundamental influence of interlayer shear interaction on the flexural behavior of laminated timber beams. The stress fields of the entirely non-composite structure show a clear separation between the two timber layers at all displacement levels. There is no shear force transfer across the contact surface because the stress contours change independently within each layer and clear stress discontinuities are seen at the interface.

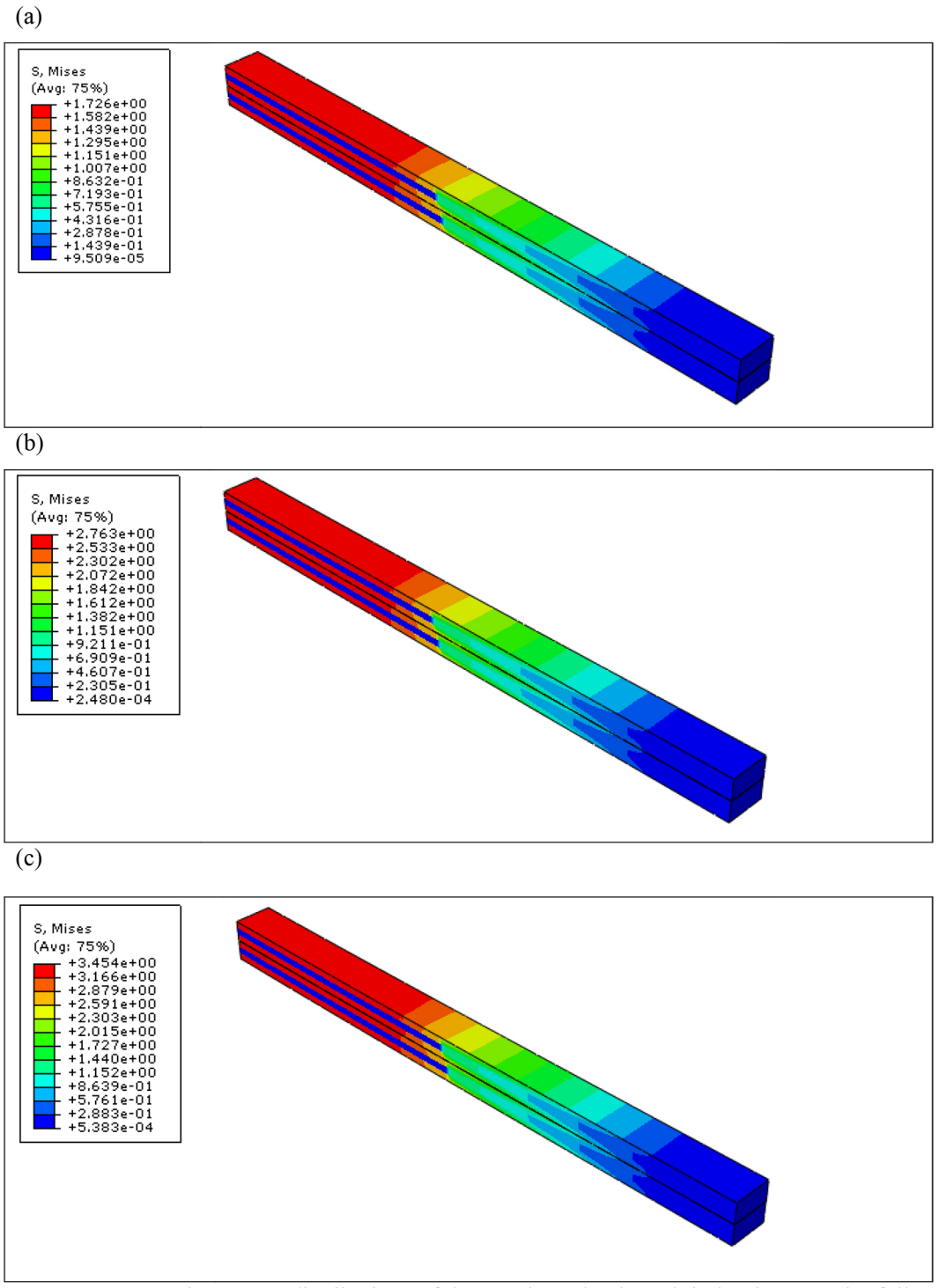

Figure 6. Von Mises stress distributions of the two-layer laminated timber beam under fully non-composite condition at different mid-span displacements: (a) 4 mm, (b) 6.4 mm, (c) 8 mm

Because of this, every layer act as a separate beam with its own neutral axis and stress gradient. This limits the effective participation of the entire section in preventing bending and results in a discontinuous stress distribution along the cross-sectional depth. While the overall stress distribution pattern maintains its segmented structure, the Von Mises stress within each layer increases proportionately with increasing mid-span displacement. An intrinsic feature of the non-composite condition is this persistent behavior, which shows that the layers continue to deform independently even at greater stress levels. Furthermore, the maximum stress observed in the fully non-composite state is

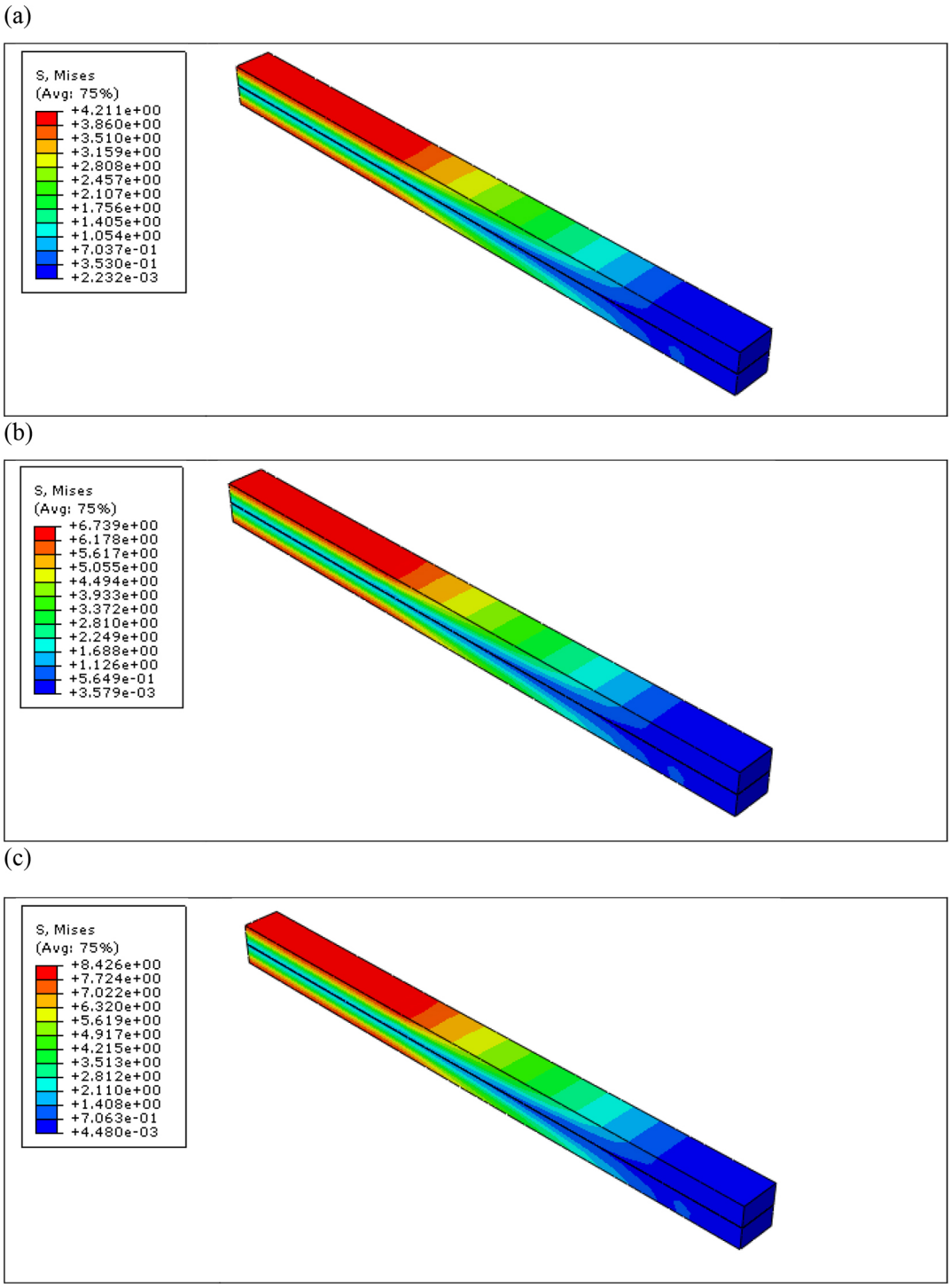

Figure 7. Von Mises stress distributions of the two-layer laminated timber beam under fully composite condition at different mid-span displacements: (a) 4 mm, (b) 6.4 mm, (c) 8 mm

substantially lower than that in the fully composite state for a given displacement level, which reflects the decreased effective bending stiffness that arises when only a portion of the cross-section contributes to load resistance.

On the other hand, a smooth and continuous stress distribution throughout the whole cross-sectional height at all displacement levels taken into consideration characterizes the fully composite configuration. Complete shear transfer between the two layers is indicated by the lack of stress discontinuities at the interface, guaranteeing displacement compatibility and allowing the beam to behave as a practically monolithic section. The stress distribution follows an approximately linear gradient from compression at the top to tension at the bottom, which is consistent with the classical bending response of a fully composite beam.

As the mid-span displacement increases, the peak stress values in the fully composite state increase accordingly, while the overall stress distribution pattern remains stable. This behavior confirms that the composite action is maintained throughout the elastic range and that the deformation mode does not change with increasing load. The higher stress levels observed in comparison with the non-composite state at the same displacement are a direct consequence of the increased flexural stiffness, as the entire cross-section is effectively mobilized to resist the applied bending moment.

A direct comparison between Figures 5 and 6 demonstrates that the degree of interlayer interaction is the governing factor controlling both the force transfer mechanism and the effective bending stiffness of the two-layer laminated timber beam. The fully composite state creates a continuous stress field and permits synchronous deformation of the entire section, while the fully non-composite state produces a segmented stress field and partial cross-sectional mobilization. This striking contrast supports the consistency and dependability of the finite element model in forecasting the elastic behavior of laminated timber beams under various contact situations, in addition to offering a clear physical interpretation of the function of interlayer shear interaction.

CONCLUSIONS

The study's overall findings show that the developed finite element model can reliably and accurately represent the elastic response of two-layer laminated timber beams. Beyond simple agreement with analytical solutions, the main contribution of this work lies in the establishment of a consistent and reproducible finite element modeling framework together with a displacement-consistent comparison strategy, enabling mechanistic interpretation of interlayer force transfer, stress redistribution, and cross-sectional mobilization – features that cannot be directly obtained from classical analytical formulations alone.The numerical findings of the successful simulation of the two hypothetical interlayer interaction conditions – completely non-composite and fully composite – show good agreement with well-established theoretical predictions. The significant difference between these two limit states makes it evident how interlayer shear interaction governs the force transfer mechanism and the beam's effective flexural stiffness. The two idealized interaction states are intentionally treated as theoretical bounding cases that define the mechanical limits of structural response, thereby providing a calibrated reference envelope for evaluating more realistic intermediate (partial interaction) configurations.

The lack of shear transfer between the layers causes a significant decrease in bending stiffness in the fully non-composite situation since each timber layer functions as a separate structural component. The entire response stays linear, suggesting that the load-bearing mechanism remains constant across the examined displacement domain, even when mid-span displacement gradually increases with applied load within the elastic range. On the other hand, the numerical model correctly simulates the behavior of a virtually monolithic section under fully composite conditions, where full shear transfer between layers allows for effective mobilization of the entire cross-section and yields the theoretically maximum flexural stiffness.

The basic distinctions between the two interaction limitations are further clarified by examining the Von Mises stress fields. In the non-composite arrangement, unconstrained interlayer slip is reflected in the distinct discontinuities at the interface and the separate development of strains within each layer. The stress field is smoothly and continuously distributed throughout the entire cross-sectional depth in the fully composite design, on the other hand, suggesting efficient force transmission and coordinated participation of both layers in the bending process.

When considered collectively, these results demonstrate that the finite element framework

created and verified in this investigation offers a solid scientific baseline for assessing the elastic behavior of two-layer laminated timber beams under idealized interlayer interaction conditions. While the present study is restricted to bounding composite limits in the linear elastic regime, the proposed framework is directly extendable to connector-based and slip-governed partial interaction models. Future work will incorporate mechanically fastened and dowel-type interlayer connections together with experimental validation to investigate intermediate composite behavior and practical design scenarios.

REFERENCES

1. Anshari B, Guan Z, Komatsu K, Kitamori A, Jung K. Explore novel ways to strengthen glulam beams by using compressed Japanese cedar. Proc. of WCTE, Riva del Garda, Italy, 2010. https://www.lajss.org/index.php/LAJSS/article/view/3682
2. Venkatarama-Reddy BV. Sustainable building technologies. Current Science, 87(7): 899–907, 2004. https://www.currentscience.ac.in/Volumes/87/07/0899.pdf
3. Puettmann ME, Wilson JB. Gate-to-gate life-cycle inventory of glued-laminated timber production. Wood and Fiber Science, 2005; 37: 99–113. https://wfs.swst.org/index.php/wfs/article/view/1374
4. Xu BH, Taazount M, Bouchaïr A, Racher P. Numerical 3D finite element modelling and experimental tests for dowel-type timber joints. Constr. Build. Mater., 2009; 23: 3043–3052. https://doi.org/10.1016/j.conbuildmat.2009.03.003
5. Feio AO, Lourenço PB, Machado JS. Testing and modeling of a traditional timber mortise and tenon joint. Materials and Structures, 2014; 47: 213–225. https://doi.org/10.1617/s11527-013-0093-8
6. Sangree RH, Schafer BW. Experimental and numerical analysis of a stop-splayed traditional timber scarf joint with key. Constr. Build. Mater., 2009; 23: 376–385. https://doi.org/10.1016/j.conbuildmat.2008.02.007
7. Nguyen PC, Tran TT, Nguyen HP, Tran TD. Nonlinear inelastic local buckling behavior of steel columns subjected to axial compression. Civil Engineering Journal, 2025; 11(9). https://doi.org/10.28991/CEJ-2025-011-09-022
8. Dejine H, Bogale M, Rynkovskaya M. Numerical analysis of the shear behavior of shallow-wide concrete beams via the concrete damage plasticity model. Civil Engineering Journal, 2025; 11(2). https://doi.org/10.28991/CEJ-2025-011-02-022
9. Kifumbi FM, Ngoma GD, Erchiqui F, Tshibangu TM. Experimental and numerical modeling of a cross-flow turbine runner made of HDPE: Experimental and numerical approach. HighTech and Innovation Journal, 2025; 6(4).
10. Forest Products Laboratory. Wood Handbook: Wood as an Engineering Material. General Technical Report FPL–GTR–190. USDA Forest Service, Madison, WI, 2010 & 2018. https://www.fpl.fs.usda.gov/documnts/fplgtr/fpl_gtr190.pdf
11. Hibbeler RC. Mechanics of Materials. 10th Edition, Pearson Education, 2017. https://www.pearson.com/en-us/subject-catalog/p/mechanics-of-materials/P200000006287
12. Möhler K. Über das Tragverhalten von Biegeträgern und nachgiebigen Verbindungsmitteln. Habilitation Thesis, TH Karlsruhe, 1956. https://www.researchgate.net/publication/292985368
13. C. O'Loinsigh, M. Oudjene, H. Ait-Aider, P. Fanning, A. Pizzi, E. Shotton, E.-M. Meghlat. Experimental study of timber-to-timber composite beam using welded-through wood dowels. In: Proceedings of Construction and Building Materials 2012; 36: 245–250. https://doi.org/10.1016/j.conbuildmat.2012.06.027
14. Abaqus, Theory Manual. Version 6.14. Providence, RI: Dassault Systèmes Simulia Corp, 2016.
15. Ross, R., Wood handbook: Wood as an engineering material. General Technical Report FPL-GTR-282. 2021, Forest Products Laboratory: Madison, WI: U.S. Department of Agriculture, Forest Service, Forest Products Laboratory. https://www.fpl.fs.usda.gov/documnts/fplgtr/fpl_gtr282.pdf